The Role of NMR in Boron Chemistry

David Reed
Department of Chemistry, University of Edinburgh, West Mains Road, Edinburgh EH9 3JJ

1 Introduction

The study of the boron hydrides and their chemistry over the past 25 years has been greatly facilitated by the rapid advances made both in X-ray crystallography and in NMR spectroscopy. The former permits the study of molecular structure in the solid state, but yields no information about the structure of, or behaviour of, materials in solution, and also needs the isolation of appropriate single crystals to permit such analysis.

NMR analysis can enable chemists to elicit structural information about molecules in solution and, in some cases, can give information about molecular dynamics (*e.g.* fluxionality).

The purpose of this review is to show, using examples as appropriate, how the range of NMR techniques now available have been used in the analysis of boron hydrides and their derivatives.

2 Applications of NMR to Boron Hydride Chemistry

Boron possesses two isotopes, namely ^{10}B and ^{11}B, both of which can be observed using NMR spectroscopy. Both possess the property known as nuclear spin, which makes such experiments possible, and in each case the spin, I, is $> \frac{1}{2}$ (see Table 1).

In common with most nuclei of $I > \frac{1}{2}$, the dominant relaxation mechanism is quadrupolar, which means that relaxation times can be quite short – for ^{11}B typical T_1 values are $< 10^{-2}$ s, though where the boron is located in a symmetrical environment this could be up to 1 s. The result of this is that ^{11}B NMR spectra tend to be made up of signals with linewidths at half the peak height, $w_{\frac{1}{2}}$, typically in the range 30—100 Hz. This problem is overcome to some extent by the nucleus possessing a reasonably large chemical shift range (*ca*, 50 ppm typically, though examples do exist outside this range). Furthermore, such linewidths do mean that only $^{1}J(^{11}\text{B}—^{1}\text{H})$ couplings are usually observed, these being in the range 80—160 Hz.

Table 1 Some properties of Boron Nuclei *vs.* Proton

Isotope	Natural % Abundance	Spin I	Resonance Frequency 2.35 T field	Relative Sensitivity *vs.* ^{1}H
^{10}B	18.83	3	9.3	0.02
^{11}B	81.17	3/2	32.1	0.165
^{1}H	99.98	1/2	100.0	1.00

Boron and proton nuclei have been used in the study of boranes, with ^{11}B being by far the more used of the two boron nuclei, both because of its sensitivity (see Table 1), and in terms of its chemical shift dispersion (it has *ca.* 3 × more Hz/ppm than ^{10}B). As mentioned earlier, the ^{11}B nucleus being quadrupolar leads to broad lines. As a result of this, some coupling information is lost, primarily $^{1}J(^{11}\text{B}—^{11}\text{B})$.

An additional problem often found with ^{11}B NMR spectroscopy is that signal overlap is not uncommon, despite the relatively large chemical shift range possible. Furthermore, the analysis of ^{1}H spectra of boranes is complicated by the coupling of the protons with the boron nuclei, particularly ^{11}B which, having $I = 3/2$, couples with the ^{1}H nucleus such that a four line multiplet of relative intensity 1:1:1:1 is observed for each proton bound to a boron. For 'bridging' hydrogens located between two boron atoms, the result is a seven line multiplet of relative intensities 1:2:3:4:3:2:1.

Some of the problems described above can be illustrated by looking at the ^{11}B, ^{11}B{^{1}H} (Figure 1), and ^{1}H (Figure 2a) spectra of the selenaborane [NEt$_3$H][B$_{10}$H$_{11}$Se].[1] The ^{11}B spectrum has all the coupling to the ^{1}H nuclei retained, whilst the ^{11}B{^{1}H} spectrum has it removed. Even in the latter case, no evidence of $^{1}J(^{11}\text{B}—^{11}\text{B})$ is apparent. Also, the ^{1}H spectrum is clearly very complex.

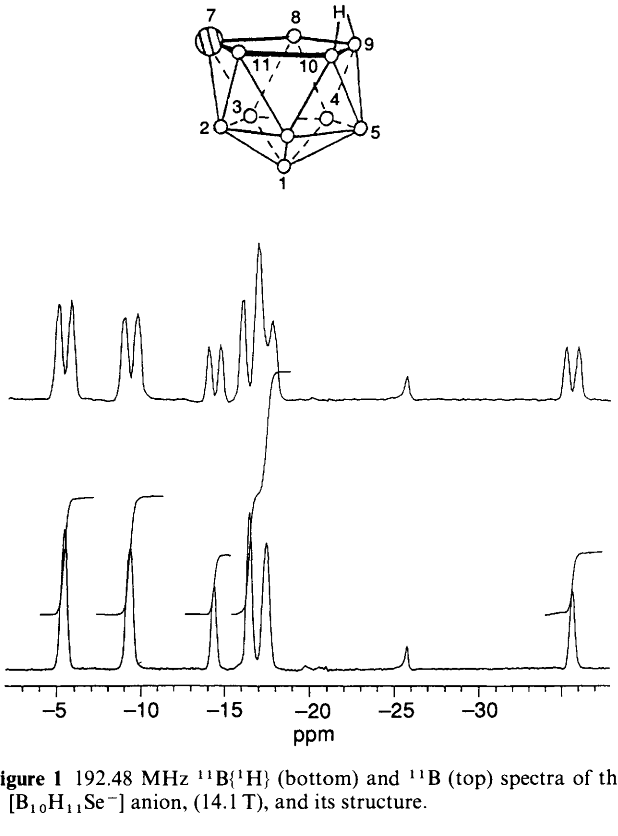

Figure 1 192.48 MHz ^{11}B{^{1}H} (bottom) and ^{11}B (top) spectra of the [B$_{10}$H$_{11}$Se^{-}] anion, (14.1 T), and its structure.

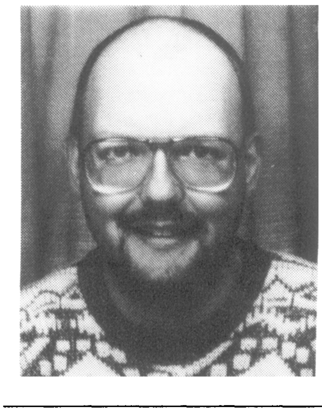

David Reed was born in Leeds, England in 1954. He obtained his B.Sc. (1975) and Ph.D. (1978) degrees from the University of Leeds, the latter degree being obtained under the supervision of Professor N. N. Greenwood and involving the study of the synthesis and characterization of metallaboranes. He then moved to the University of Strathclyde, where he worked on electrochemical studies of boron compounds. Since 1981 he has been associated with the High Field NMR Centre at the University of Edinburgh, where he has particular interests in using high field NMR to study solution structures and properties of both main-group and transition-metal cluster compounds.

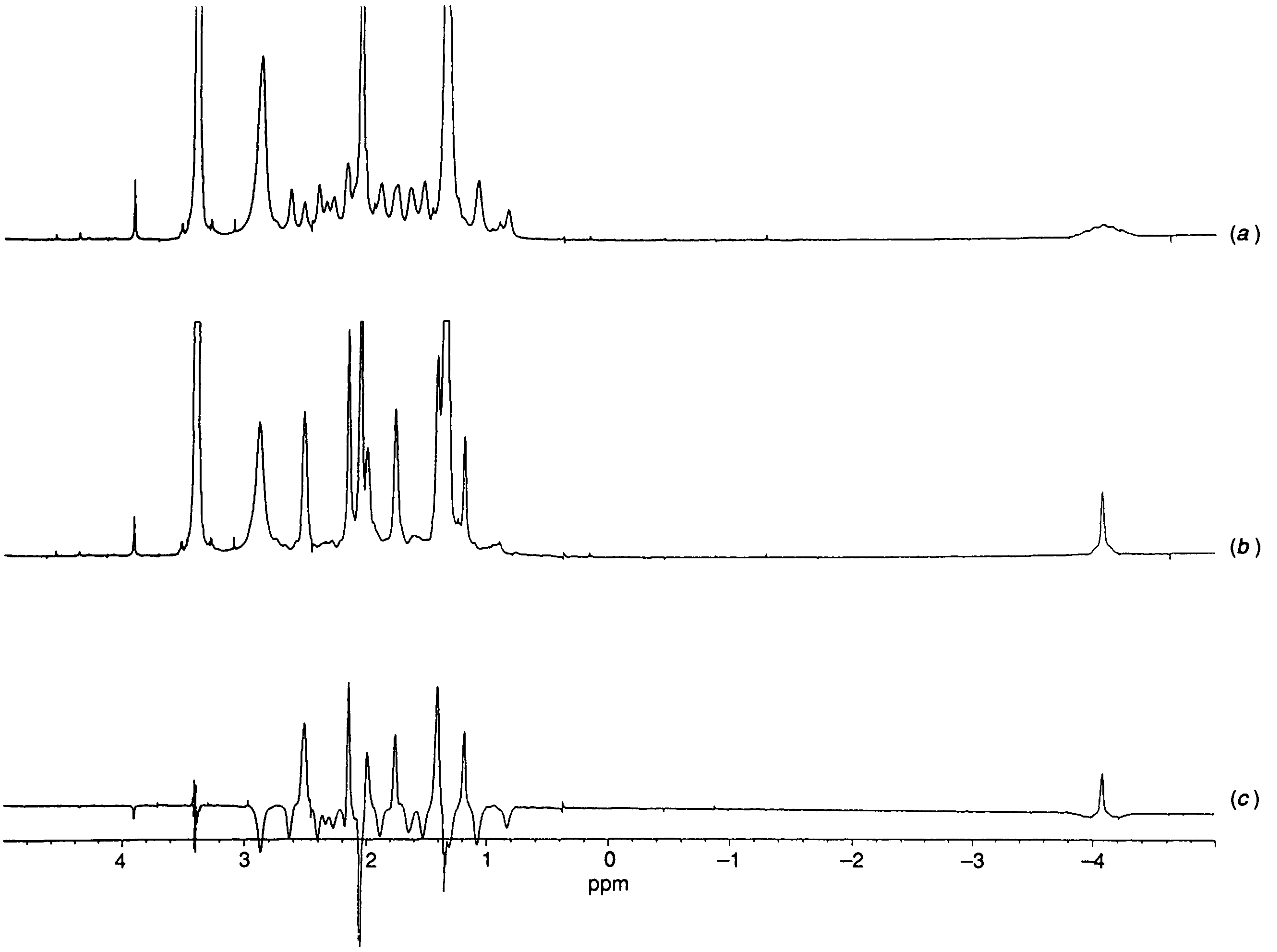

Figure 2 (a) ^1H spectrum of $[NEt_4][B_{10}H_{11}Se]$; (b) $^1H\{^{11}B\}$ spectrum of $[NEt_4][B_{10}H_{11}Se]$; (c) (b) − (a).

Table 2 Comparison of ^1H and ^{11}B resonance frequencies at different magnetic field strengths (Tesla)

Field Strength (T)	Resonance Frequency ^{11}B (MHz)	Resonance Frequency ^1H (MHz)
2.35	32.1	100
4.70	64.2	200
8.46	115.5	360
14.10	192.5	600

Broad band boron decoupling results in a much simplified ^1H spectrum (Figure 2b), with all the cage protons giving rise to singlet signals, though these are partly hidden by signals arising from the organic cation. Such difficulties can be minimized by obtaining a difference spectrum (Figure 2c).

The spectra described above do not yield much information regarding B—B or B—H connectivities, and a complete analysis of such a system would require such information. There have been some technical advances in recent years which have greatly boosted such studies:

(i) The development of superconducting magnets has resulted in magnetic field strengths as high as 14.1 Tesla (to date). Increasing magnetic field strength has two major benefits, namely increased sensitivity and increased dispersion of signals. Table 2 shows the comparison of magnetic field strength (Tesla) with ^1H and ^{11}B resonance frequencies (MHz).

(ii) During the past 15 years or so there has been a rapid increase in the use of pulse sequences. Some of these have resulted in the development of two-dimensional NMR, an idea which was first proposed by Jeneer,[2] and first demonstrated by Ernst.[3] Since that time innumerable variations of such experiments have been described, primarily involving correlation of homonuclear or heteronuclear spin–spin couplings and homonuclear or heteronuclear NOE effects.[4]

In the NMR study of boron hydrides, the main objective would be to establish B–H and B–B connectivities with relevant signal assignment, thereby assisting in structure elucidation. The determination of such information can be effected by a combination of $^{11}B/^1H$, $^{11}B/^{11}B$, and $^1H/^1H$ correlation experiments, as appropriate.

To illustrate how such experiments can be used, the selenaboranes $[B_{10}H_{11}Se^-]$[1] and $[B_9H_9Se_2]$[5] will be examined in detail. In both cases comprehensive assignment was achieved with $^{11}B/^1H$ and $^{11}B/^{11}B$ correlation experiments. The problem with the anionic species was one of assignment of the signals, the structure having been determined crystallographically. The diselenaborane was studied because there was a question about the molecular structure, with two possibilities as shown in Figure 3.

Correlation of ^1H signals with ^{11}B signals can be effected in either of two ways, namely *via* the two-dimensional 'hetcor' experiment or by one-dimensional selective $^1H\{^{11}B\}$ experiments. The former has not been extensively utilized by boron chemists, though the first illustrations of the application of two-dimensional techniques to boron hydrides were shown using this type of experiment.[6,7] The first example given was of its application to the carbaborane $C_2B_5H_7$,[6] which demonstrated the potential of the experiment, and this was followed up by two papers showing the application to decaborane(14).[7,8]

The result of such an experiment is a plot which correlates chemical shifts of the ^1H nuclei, $\delta(^1H)$, with those of the boron nuclei, $\delta(^{11}B)$. Such information can be presented in either of two ways, namely as a stacked plot (as indicated in Figure 4a) or as a contour plot (as shown in Figure 4b). In practice, the former is of little value, as it is not easy to extract the chemical shift

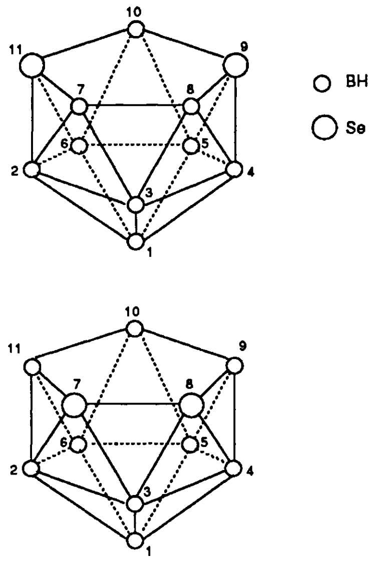

Figure 3 The two possible structures of [$B_9H_9Se_2$].

information from such a presentation, while the contour plot provides an easy-to-read presentation of such data. The experiment uses delays which are derived from the value of J(X–H) (X = ^{11}B in this case) and as a result, the main problem associated with this technique is the difference in ^1J(B–H) values between terminal (*exo*) B–H nuclei and bridging B–H–B nuclei (*ca.* 140 Hz and *ca.* 40 Hz respectively). Experimental parameters can be modified to take this into account, but not always successfully: sometimes responses deriving from bridging nuclei are weaker than ideal.

Such an experiment was used for the correlation of ^{11}B and ^{1}H signals in [$B_9H_9Se_2$], this having no bridging protons. The resulting plot, shown in Figure 5, allows clear correlation between the ^{1}H and ^{11}B chemical shifts in this case.

The second method of correlating ^{1}H and ^{11}B signals, and by far the most popular in practice, is *via* ^{1}H observation with selective ^{11}B decoupling. Many modern FT instruments possess the capability for this type of experiment. The experiment is carried out by observing ^{1}H while simultaneously irradiating at a frequency corresponding to an individual ^{11}B signal. A spectrum is also acquired where decoupling power has been applied at an off-resonance position, thus providing an effectively undecoupled spectrum. Subtraction of the latter from the former provides a decoupling difference spectrum. Such an experiment is repeated for all the ^{11}B frequencies determined from the ^{11}B spectra. The results of this type of experiment for the [$B_{10}H_{11}Se^-$] anion are shown in Figure 6. Particularly noteworthy is the clear bridging proton response on decoupling at the boron frequency corresponding to the ^{11}B signal at δ − 17.6 ppm.

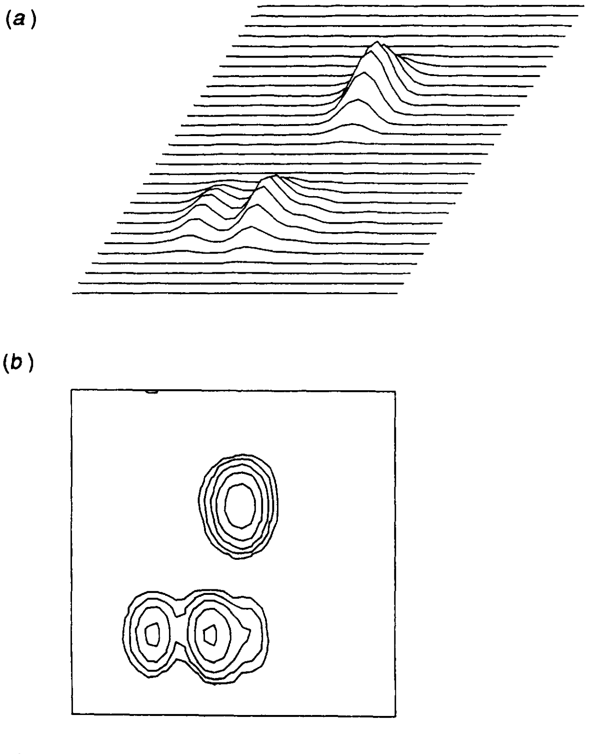

Figure 4 Examples of (a) a stacked plot two-dimensional spectrum and (b) the same data presented as a contour plot.

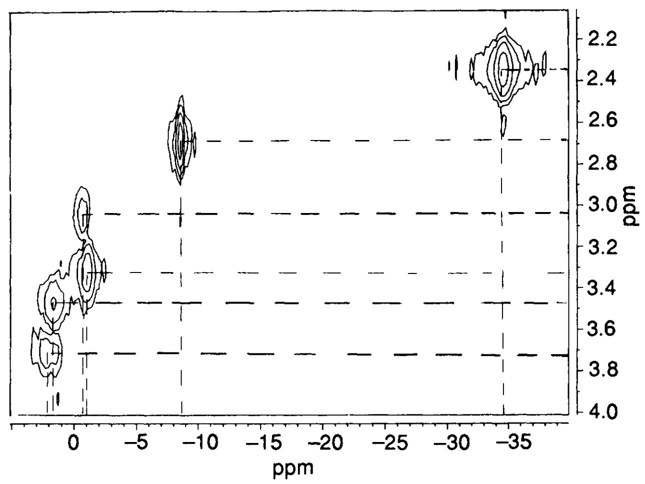

Figure 5 An ^{11}B/^{1}H two-dimensional correlation experiment on [$B_9H_9Se_2$] carried out at 8.46 T (360.1 MHz for ^{1}H; 115.5 MHz for ^{11}B).

Boron–boron connectivity data can be extracted by using perhaps the most commonly applied of the two-dimensional NMR experiments that have emerged over the last fifteen years, namely the COSY experiment (from COrrelation SpectroscopY). The use of ^{11}B–^{11}B two-dimensional correlation spectroscopy was initially demonstrated by Grimes *et al.*, showing its application to the cobaltaborane [6-CpCo(B_9H_{13})] and the carbaborane [2,3-(C_2H_5)$C_2B_4H_6$].[9] This was followed by a more comprehensive overview of its applications, as well as of some limitations.[10] Similar conclusions were drawn from other work described at that time.[11]

The examples quoted in these papers led to a number of observations about the application of ^{11}B COSY which, for brevity, will be outlined here prior to more detailed discussion of some examples.

(i) There is no evidence for couplings betweeen non-adjacent boron nuclei.

(ii) Boron nuclei connected by bridging hydrogens are less likely to show COSY responses, although examples do exist where such responses are found.

(iii) Where boron nuclei exhibit shorter relaxation times it is more difficult to get good COSY spectra.

(iv) Boron signals often overlap coincidentally, leading to interpretation problems.

Some early examples of ^{11}B COSY experiments suggested that boron nuclei linked by bridging hydrogens did not exhibit coupling[9,11] though contradictions to this idea were quickly found, namely [2-(C_2H_5)CoB_4H_8] and [*nido*-1,2,3-(C_6Me_6)Fe-(C_2H_5)$_2C_2B_3H_5$].[10]

The result of a COSY experiment carried out on [$B_{10}H_{11}Se^-$] is shown in Figure 7. Analysis of such data is relatively straightforward. The one-dimensional spectrum is mirrored along the diagonal, while those borons which are coupled may give rise to off-diagonal responses (cross peaks) at (Bx,By) and (By,Bx).

The analysis of the data in Figure 7 was greatly assisted by the

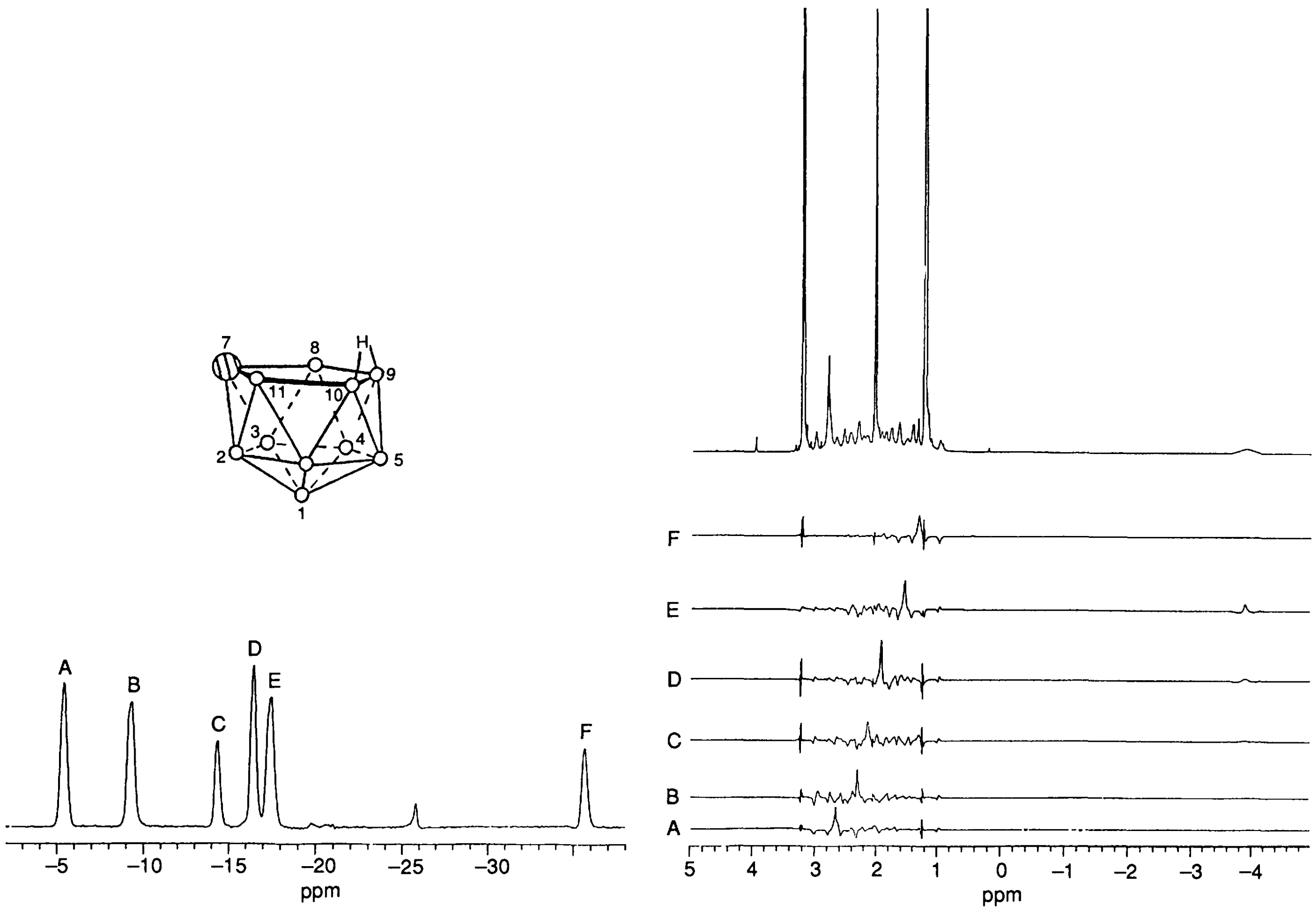

Figure 6 A series of selective $^1H\{^{11}B\}$ difference spectra for $[B_{10}H_{11}Se^-]$, carried out at 14.1 T. An $^{11}B\{^1H\}$ spectrum shows the ^{11}B decoupling sites.

fact, derived from the selective $^1H\{^{11}B\}$ data, that the ^{11}B signal due to B(9,10) is found at δ − 17.6. Also, of the two signals possessing relative area one, only that at δ − 14.6 shows coupling to B(9,10), and hence must derive from B(5). Thus the signal at δ − 35.6 must arise from B(1). The highest frequency signal, at δ − 5.6, shows coupling to all others, and is thus due to B(4,6). The signal at δ − 9.2 couples to that of B(9,10), and must arise from B(8,11), leaving the last signal at δ − 16.3 being due to B(2,3). One noteworthy feature of the COSY is that an expected correlation between B(2,3) and B(8,11) has not been observed; for this there is no apparent explanation. Table 3 summarizes the ^{11}B and ^1H assignments observed for $[B_{10}H_{11}Se^-]$ derived from the experiments outlined.

The one-dimensional ^{11}B and $^{11}B\{^1H\}$ spectra of $[B_9H_9Se_2]$ are shown in Figure 8, with six boron environments of relative intensities 1:2:2:2:1:1. These data would be consistent with either of the structures in Figure 3, both of which possess a plane of

Table 3 Assignments of the ^{11}B and ^1H NMR spectra of the $[B_{10}H_{11}Se^-]$ anion

$\delta(^{11}B)$	$\delta(^1H)$	Assignment
− 5.6	2.37	4,6
− 9.2	2.05	8,11
− 14.6	1.83	5
16.3	1.67	2,3
− 17.6	1.26	9,10
− 35.6	1.05	1
	− 4.11	bridge (9,10)

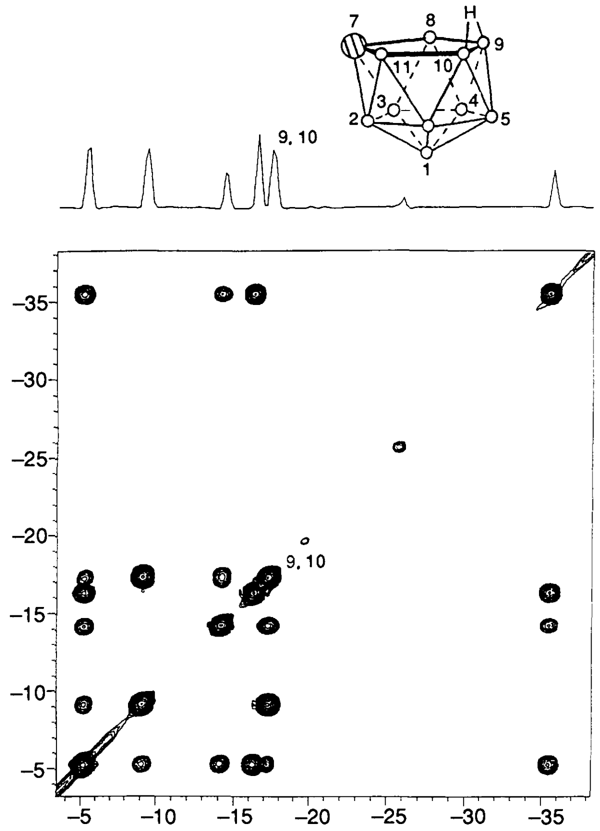

Figure 7 An ^{11}B COSY Experiment on $[B_{10}H_{11}Se^-]$, carried out at 14.1 T.

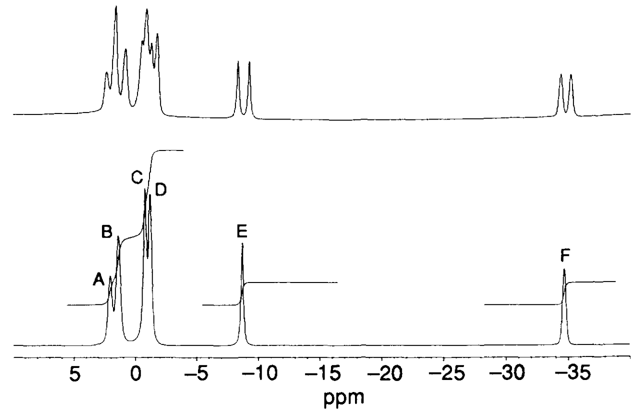

Figure 8 192.48 MHz $^{11}B\{^1H\}$ (bottom) and ^{11}B (top) NMR spectra of $[B_9H_9Se_2]$ carried out at 14.1 T.

symmetry through B(1), B(3), and B(10). The ^{11}B COSY spectrum of this molecule (Figure 9) provided both signal assignment and structural determination, the latter on the basis of the proposal that non-adjacent ^{11}B nuclei do not give rise to cross peaks.

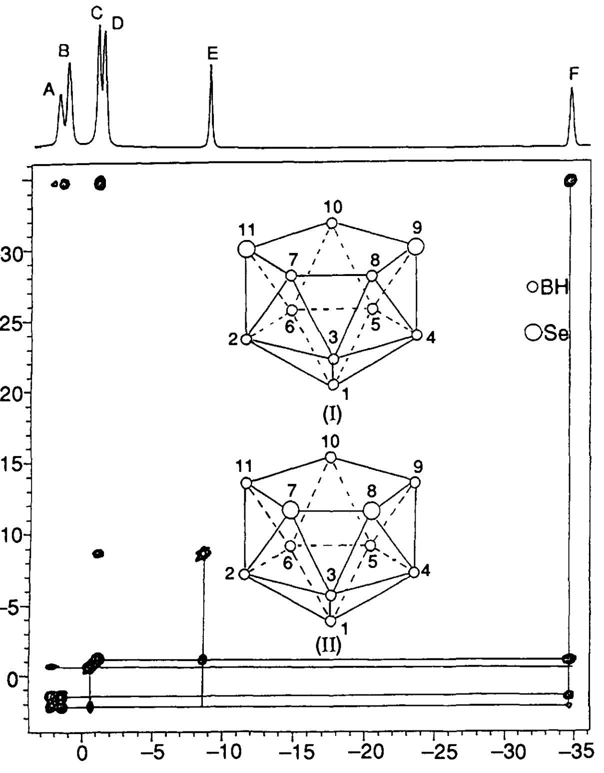

Figure 9 An ^{11}B COSY experiment on $[B_9H_9Se_2]$ carried out at 14.1 T.

Thus if (I) were the correct structure, then B(1), B(3), and B(10) should each display 3,2, and 2 correlations respectively. Were the structure consistent with (II), then B(1), B(3) and B(10) should each show 3,3, and 1 connectivities respectively. Figure 9 shows that two of the area 1 signals, namely A and F, have cross peaks associated with them, whilst E only shows one cross peak. Thus (II) appears to be the structure.

From this it is clear that E is the signal from B(10), meaning D must derive from B(5,6). Signal D in turn couples with F, so F must arise from B(1). Signal F also couples to B, which must be ascribable to B(2,4), leaving C as B(7,8). Thus $[B_9H_9Se_2]$ adopts structure II, and its ^{11}B and ^{1}H assignments are summarized in Table 4.

Table 4 Assignments of the ^{11}B and ^{1}H NMR spectra of $[B_9H_9Se_2]$

$\delta(^{11}B)$	$\delta(^{1}H)$	Assignment
2.1	3.63	3
1.6	3.48	2,4
− 0.6	3.02	7,8
− 1.0	3.33	5,6
− 8.6	2.68	10
− 34.6	2.33	1

A general point, alluded to earlier, is that often in ^{11}B COSY experiments cross peaks do not show up. In some cases there is no apparent reason (as in the example earlier with $[B_{10}H_{11}Se^-]$). Sometimes, however, such behaviour can be rationalized in terms of the rapid relaxation properties exhibited by some ^{11}B nuclei. Such quadrupolar induced relaxation can be made less efficient by sample heating, thereby improving chances of success. However, the thermal instability of many compounds often precludes this measure.

In many cases the techniques discussed so far are adequate for the complete assignment of ^{11}B and ^{1}H resonances. Occasionally, however, they are not adequate. Problems of rapid ^{11}B relaxation, 'missing' cross peaks or overlapping ^{11}B signals occur all too often. Such problems can be overcome in some cases by the use of ^1H–^1H COSY with simultaneous broad band ^{11}B decoupling, the first application of which was to the rhodaborane $[5\text{-}(C_5H_5)\text{-}5\text{-}Rh\text{-}nido\text{-}B_9H_{13}]$, Figure 10.[13] This example highlighted a number of useful features which supplement data gathered from other experiments (Figure 11). Thus, in addition to showing the presence of ^3J(H–B–B–H) between *exo* cage protons, couplings between bridging protons and *exo* protons were also shown, including those involving the Rh–H–B. A number of problems relating to this type of experiment were also defined. For example, the ^{11}B chemical shift range is often several thousand hertz, and it may not be possible to effect full decoupling over the whole chemical shift range as a result. This problem is, of course, exacerbated at higher field strengths. Also, other ligands which contain organic components may be present in the molecule: these tend to give much sharper signals in the ^1H spectrum than do decoupled cage protons. This can mean 't_1 noise' interfering with the resulting ^1H–^1H COSY, this problem showing up as streaks along one of the two dimensions.

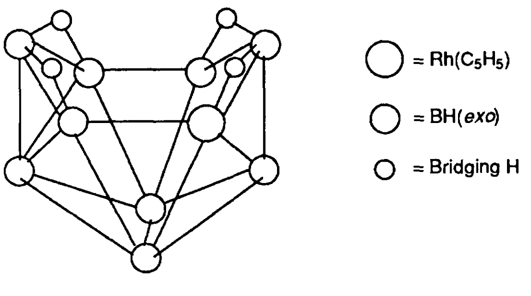

Figure 10 Structure of $[5\text{-}(C_5H_5)\text{-}5\text{-}Rh\text{-}nido\text{-}B_9H_{13}]$.

Finally, it would be inappropriate to ignore the uses of NMR in looking at fluxional processes in boron hydride derivatives.

Bridge/*endo* hydrogen fluxionality was studied for the systems $[B_9H_{13}L]$ ($L = SMe_2$, SEt_2, MeCN, $(Me_2N)_2CN$, BH_3CN^-, SCN^-).[14,16] Of these, the structure of the CH_3CN derivative has been determined crystallographically.[17] Interestingly, the NMR properties of these were shown to differ between the neutral $[B_9H_{13}L]$ complexes and the anionic $[B_9H_{13}L]^-$ examples with the notable exception of the neutral $(Me_2N)_2CN$ derivative, whose properties were like those of the anionic species quoted.[15] The room temperature ^{11}B and $^{11}B\{^1H\}$ spectra of $B_9H_{13}SEt_2$ (Figure 12) are typical of the neutral species, whilst those of $[B_9H_{13}\ NCS^-]$ (Figure 13) are typical of the anionic derivatives. In the former case, the ^{11}B spectrum comprises six doublets, labelled A—F. In the latter there are five

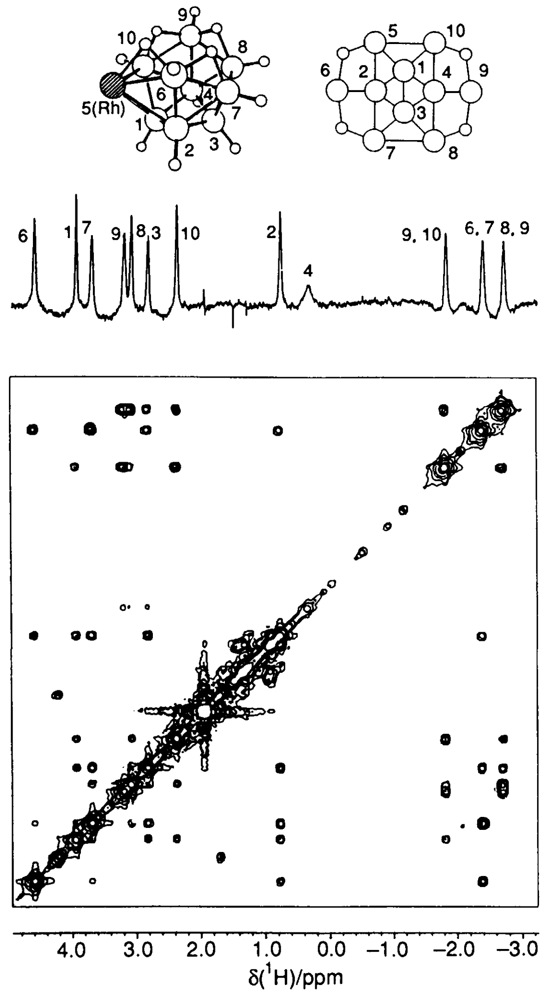

Figure 11 400 MHz ^{1}H COSY (^{11}B decoupled) experiment on [5-(C_5H_5)-5-Rh-*nido*-B_9H_{13}].
(Reproduced from reference 13.)

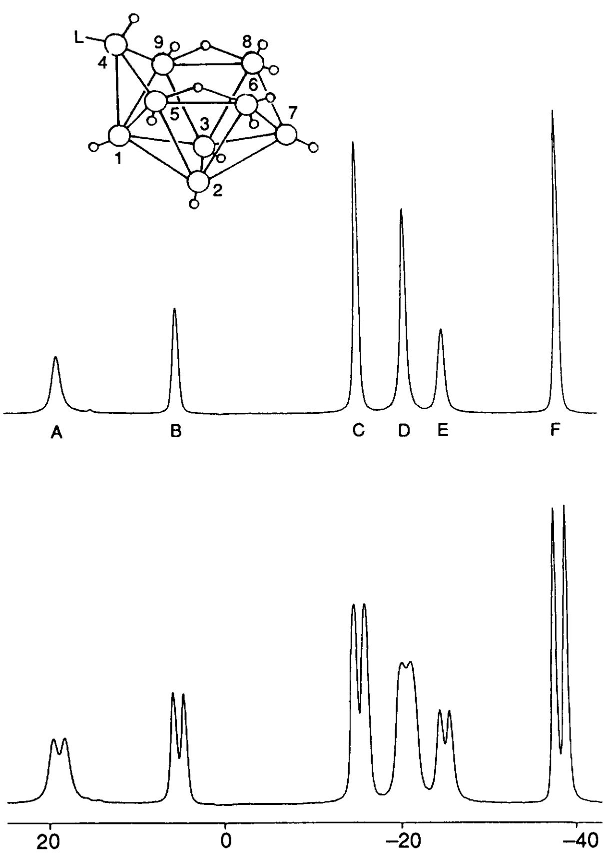

Figure 12 115.5 MHz ^{11}B (botom) and ^{11}B{^{1}H} (top) NMR spectra of [$B_9H_{13}SEt_2$] (8.46 T), and its structure.

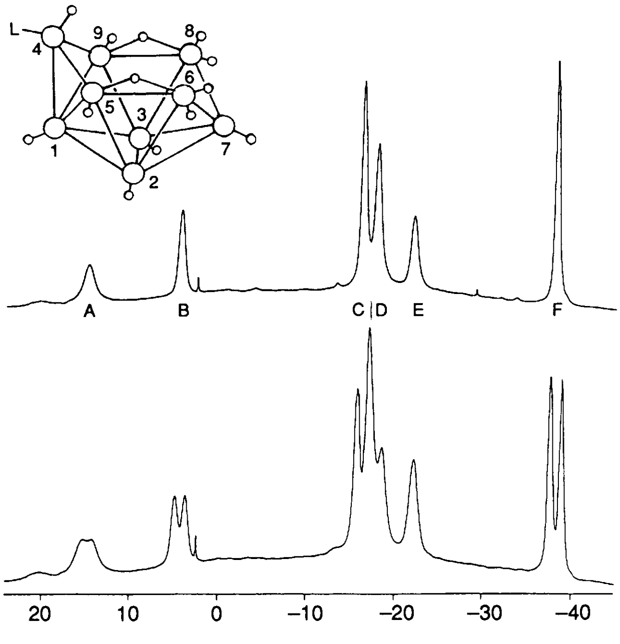

Figure 13 115.5 MHz ^{11}B (bottom) and ^{11}B{^{1}H} (top) NMR spectra of [$B_9H_{13}NCS^-$] (8.46 T).

doublets and one singlet (signal E). In both cases signal E was ascribed to B(4), which was subsequently confirmed by ^{11}B COSY experiments.[11] The differences in the ^{11}B spectra of the neutral and anionic species were taken to imply that the proton on B(4) was fluxional with the bridging protons in the latter (anionic) cases, but not so in the neutral. This was supported by ^{1}H{^{11}B} NMR data (Figures 14 and 15), which show distinct signals corresponding to bridging hydrogens at *ca.* δ − 3.50 in the neutral cases, whereas in the anionic examples a broad signal corresponding to 5 protons was found at *ca.* δ − 1.4. Thus, the anionic examples quoted showed fluxionality between the two bridging hydrogens and the '*endo*' hydrogens on B(4), B(6), and B(8), whereas the static form was observed for the neutral derivatives. The static form of the ^{1}H{^{11}B} spectra of the NCS$^-$ derivatives was reached if the data were acquired at 203 K. Thus the energy barrier to such intramolecular hydrogen exchange processes was shown to be dependent on the ligand used.

A rather different type of temperature dependent phenomenon was described for the *closo* metalladicarbaborane derivative [1-Ph-3-(π-C_9H_7)-3,1,2-*closo*-$CoC_2B_9H_{10}$], whose crystallographically determined structure is given in Figure 16.[18] In this example the interest lay in the behaviour of the phenyl and the indenyl ligands. The variable temperature ^{1}H NMR spectra, showing the aromatic region, are given in Figure 17. The spectrum recorded at 298 K showed signals which were consistent with seven indenyl protons but only three phenyl protons. Subsequent low temperature experiments showed the presence of two further signals, which were readily ascribable to *ortho* protons from the phenyl ring. One of these, labelled A, moved significantly to lower frequency with decreasing temperature. In addition the signal labelled B also moved to lower frequency as the temperature decreased. The explanation of such behaviour is that the phenyl group is undergoing a slowing of rotation around the C(1)–C(11) axis with decreasing temperature. Thus, at room temperature the rate of exchange of the *ortho* protons will be about the same as their ^{1}H NMR separation in Hz. This results in coalescence of the signals which, when they are widely separated, means they will 'vanish'. On cooling, their rate of

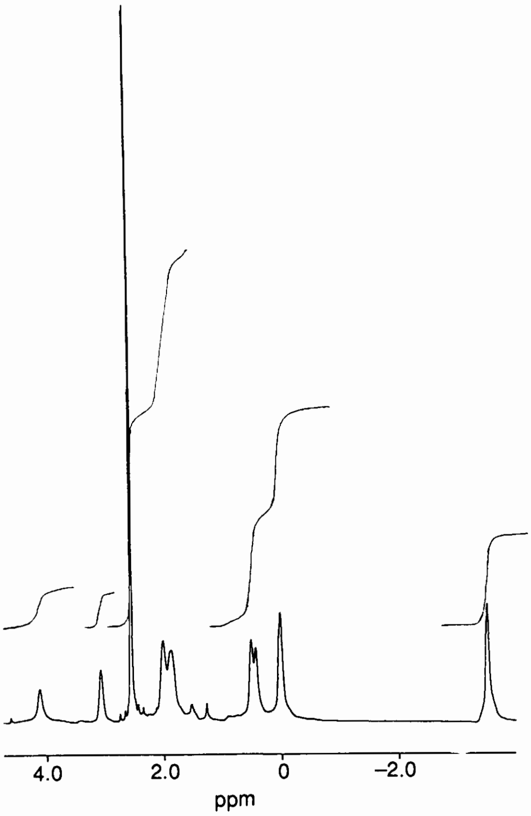

Figure 14 360.13 MHz $^1H\{^{11}B\}$ NMR spectrum of $[B_9H_{13}SEt_2]$ (8.46 T).

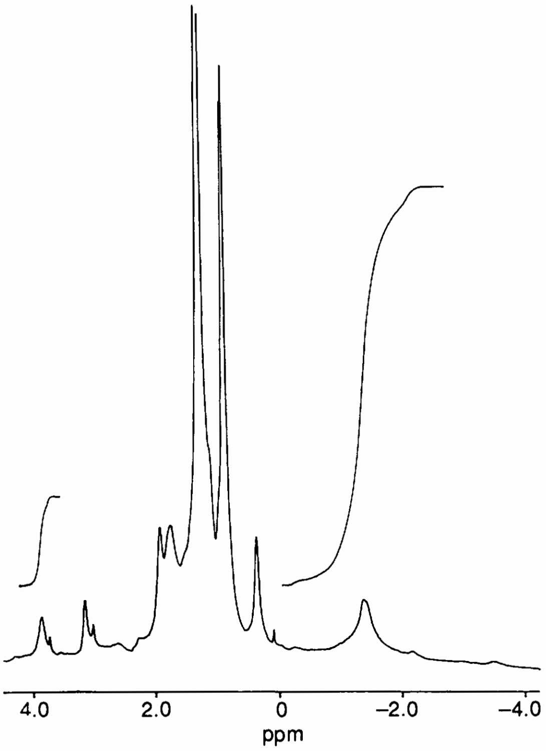

Figure 15 360.13 MHz $^1H\{^{11}B\}$ NMR spectrum of $[B_9H_{13}NCS^-]$ (8.46 T).

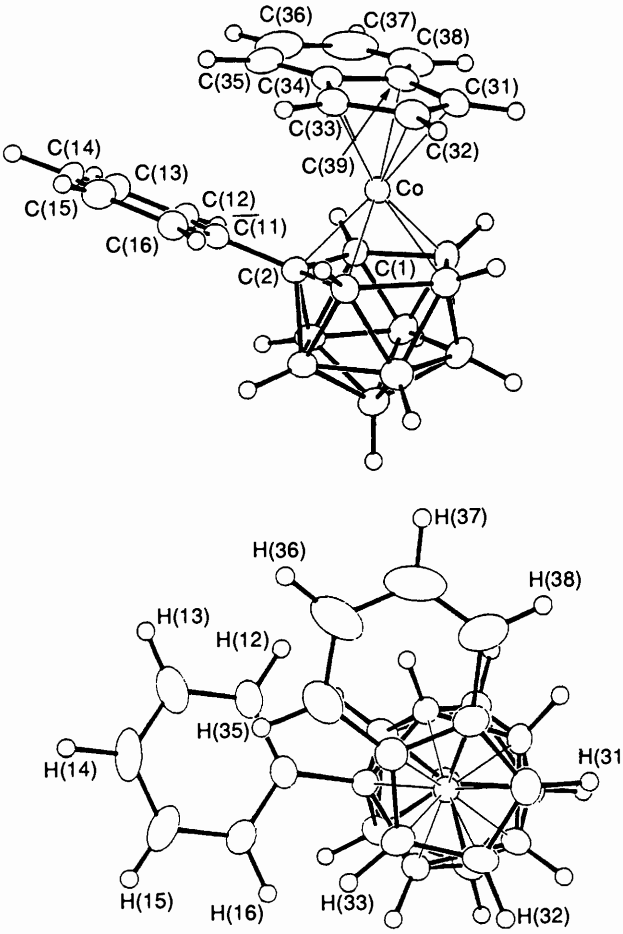

Figure 16 Structure of $[1\text{-Ph-}3\text{-}(\pi\text{-}C_9H_7)\text{-}3,1,2\text{-}closo\text{-}CoC_2B_9H_{10}]$.

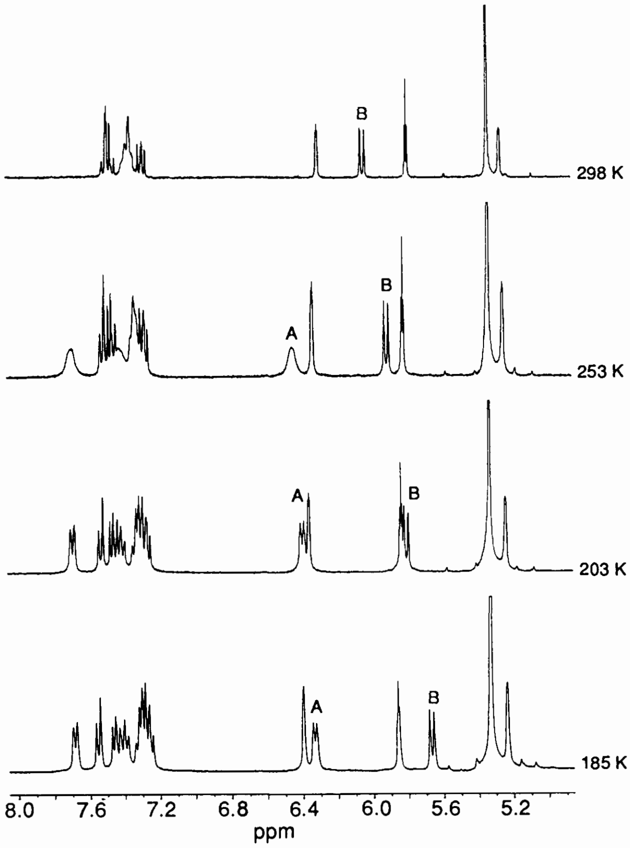

Figure 17 Variable temperature ^1H NMR spectra of $[1\text{-Ph-}3(\pi\text{-}C_9H_7)\text{-}3,1,2\text{-}closo\text{-}CoC_2B_9H_{10}]$.

exchange has become less, so the individual signals can be observed The low frequency shifts of A and B can be explained if the preferred low temperature conformation is consistent with the crystal structure Thus H(12) and H(35) (A and B respectively) are each sitting above aromatic π systems, and are consequently deshielded

3 Summary

The previous section has shown how various NMR techniques have been applied to a selection of boron hydride derivatives It has shown that different types of data can be extracted from such systems Thus, signal assignments can be carried out by use of appropriate correlation experiments It was also demonstrated that where structural data were not available, such information could be deduced from suitable correlation experiments, using the specific example of $[B_9H_9Se_2]$ Additionally, examples were given that showed how data could be extracted about systems which exhibit dynamic processes in solution

NMR can therefore be shown to both supplement and, in suitable cases, substitute for *X*-ray crystallographic studies

Acknowledgements I would like to thank Dr A R Butler for advice and discussion about the manuscript, Drs T R Spalding and J H Morris for provision of many of the samples discussed, and the S E R C for the provision of both the 8 5 T and 14 1 T instruments

4 References

1 D Reed, G Ferguson, B L Ruhl, O Ni Dhubhghaill, and T R Spalding, *Polyhedron*, 1988, **7**, 117
2 J Jeneer, Ampere International Summer School, Basko Polje, Yugoslavia (1971), unpublished
3 W P Aue, E Bartholdi, and R R Ernst, *J Chem Phys* , 1976, **64**, 2229
4 Several good reviews have been published, *e g* G A Morris, *Magn Reson Chem* , 1986, **24**, 371, R Benn and H Gunther, *Angew Chem Int Ed Engl* , 1983, **22**, 350
5 D Reed, T R Spalding, paper in progress
6 D C Finster, W C Hutton, and R N Grimes, *J Am Chem Soc* , 1980, **102**, 400
7 I Colquhoun and W McFarlane, *J Chem Soc Dalton Trans* , 1981, 2014
8 D P Burum, *J Magn Reson* , 1984, **59**, 430
9 T L Venable, W C Hutton, and R N Grimes, *J Am Chem Soc* , 1982, **104**, 4716
10 T L Venable, W C Hutton, and R N Grimes, *J Am Chem Soc* , 1984, **106**, 29
11 D Reed, *J Chem Research (S)*, 1984, 198
12 K Base, *Collect Czech Chem Commun* , 1983, **48**, 2593
13 X L R Fontaine and J D Kennedy, *J Chem Soc Chem Commun* , 1986, 779
14 G B Jacobsen, J H Morris, and D Reed, *J Chem Soc Dalton Trans* , 1984, 415
15 D G Meina, J H Morris, and D Reed, *Polyhedron*, 1986, **5**, 1639
16 G B Jacobsen, D G Meina, J H Morris, C Thomson, S J Andrews, D Reed, A J Welch, and D F Gaines, *J Chem Soc Dalton Trans* , 1985, 1645
17 F E Wang, P G Simpson, and W N Lipscomb, *J Chem Phys* , 1961, **35**, 1335
18 Z G Lewis, D Reed, and A J Welch, *J Chem Soc Dalton Trans* , 1992, 731